Ring-modulator-based RoF system with local SSB modulation and remote carrier reuse

Zhenzhou Tang, Jing Zhang, Shilong Pan✉, Gunther Roelkens and Dries Van Thourhout

A full-duplex radio-over-fibre (RoF) system based on an integrated silicon ring modulator is proposed and demonstrated. For the downstream link, a coherent dual-wavelength laser source is coupled to a silicon ring modulator in the central office (CO). Since only one of the optical carriers in the dual-wavelength laser source is aligned to the resonance of the ring modulator, a single sideband (SSB) modulated optical downstream signal is obtained, which is able to combat the power fading introduced by the fibre dispersion. Besides, for the upstream link, the unmodulated optical carrier in the SSB-modulated optical downstream signal is reused by using an optical filter in the remote radio head. After being modulated by the upstream data, the optical upstream signal is transmitted back to the CO. A proof-of-concept experiment is carried out. Error vector magnitudes of 21-GHz downstream and 10-GHz upstream signals are measured, which confirms that the proposed architecture is a promising low-cost solution for future high-speed wireless communication systems.

Introduction: Next-generation mobile communication systems are expected to provide massive device connectivity, high system capacity and large service coverage with low latency and sustainable cost [1]. Radio-over-fibre (RoF) technology, thanks to its simple remote radio head (RRH) structure, is regarded as one of the most promising solutions. In the RoF system, the analogue RF signal is directly generated in the central office (CO) and transmitted to the RRH via low-loss optical fibre. Since all the complex and expensive components can be shifted to the CO, a unified platform for massive RRH connection, centralised signal processing, and dynamic resource allocation becomes possible [2].

Although various RoF systems have been reported to realise high-capacity communications at the millimetre wave or even THz band [3–6], the cost, complexity and power consumption of the RoF system still need to be further reduced in response to the increasing number of connected devices. To do so, several approaches can be employed. For instance, making use of the advantage offered by photonic integration technologies in terms of manufacturing low-cost devices in high volume, photonic integrated devices such as directly-modulated vertical cavity surface-emitting lasers (VCSELs) [7], III-V-on-silicon RoF transceivers [8, 9], ring resonators for optical filtering [10, 11] and RF frequency upconverters based on GeSi electro-absorption modulators [12] have been reported in order to reduce the cost of an RoF system. In addition, optical single sideband (SSB) modulation is a promising scheme to relieve the burden of signal processing for dispersion compensation in the receiver since it can combat the power fading introduced by the fibre dispersion. Compared with SSB modulation based on optical filtering [13] and a dual-drive Mach-Zehnder modulator (MZM) driven by a pair of quadrature signals [14], combining an unmodulated carrier with a modulated one is widely employed, due to the advantage of flexible operation and broad bandwidth [15, 16]. However, a sophisticated transmitter based on sidebands separation, modulation and recombination is usually used [15], which makes the system bulky and costly. Even though the transmitter can be simplified by using a free-running laser source [16], additional carrier phase estimation should be applied, which also increases the complexity of the receiver.

In this Letter, to combine the above two techniques in a simple structure, we propose a novel full-duplex RoF system with three key features: (a) a compact and low-cost silicon photonic integrated ring modulator with a bandwidth of 15 GHz is used for the local electro-optic modulation of the downstream data; (b) since the modulation efficiency is sensitive to the wavelength of the optical carrier sent to the ring modulator, an SSB-modulated signal is easily obtained (without sidebands separation and recombination), when two coherent optical carriers, of which one is aligned to the resonance of the ring modulator, simultaneously go through the modulator; (c) remote wavelength reuse by using an optical filter to select the unmodulated optical carrier in the SSB-modulated signal in the RRH, which avoids the need for extra light sources and their drivers in the RRH. A proof-of-concept experiment is carried out. The error vector magnitudes (EVMs) of the 21-GHz downstream and 10-GHz upstream signals are measured. The sensitivity of the EVM to the bias of the ring modulator is also studied.

Device and system: Fig. 1*a* shows a microscopic image of the integrated PN-doped ring modulator together with two grating couplers for the coupling of the light. The radius of the ring resonator is about 7.5 μm and it is fabricated in imec's iSIPP25G platform. Fig. 1*b* shows the measured normalised static transmission response of the ring modulator. As can be seen, the ring modulator has resonances around 1542.16, 1554.96 and 1567.94 nm, respectively, with a free spectral range of about 12.8 nm and an extinction ratio (ER) of about 12.6 dB (@ 1554.96 nm). To measure the DC properties of the modulator, the bias voltage applied to the ring modulator is changed from −2 to 0.5 V. The measured result is shown in Fig. 1*c*. The resonant wavelength shifts with the change of the bias voltage, and the ER is about 10 dB for a 2.5 Vpp voltage swing. Small signal characterisation is also carried out by using an electrical vector network analyser (Agilent N5247A), with the result presented in Fig. 1*d*. The electro-optic modulation bandwidth of the ring modulator, as can be seen, is 15 GHz at −1 V bias.

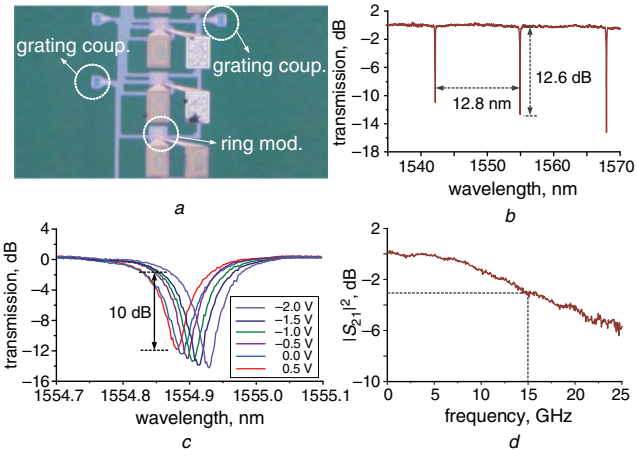

Fig. 1 *Ring modulator and characterisation*
a Microscopic image of the ring modulator
b Transmission response of the ring modulator
c Resonant wavelength shift versus bias increasing from −2 to 0.5 V
d Normalised $|S_{21}|^2$ response of the ring modulator

Based on the integrated silicon ring modulator, a full-duplex RoF system is proposed, as shown in Fig. 2. In the CO, a coherent dual-wavelength (dual-λ) laser source is used. Here, in our experiment, a carrier-suppressed-double-sideband (CS-DSB)-modulated signal serves as the dual-λ laser source. To do so, a tunable optical carrier (Santec TSL-510) with a power of 10 dBm is firstly sent to a commercially-available 10-GHz MZM. When a single-tone RF signal with a frequency of $f_D/2$ is applied to the MZM and the DC voltage is adjusted to bias the MZM at the null transmission point, a dual-λ laser source with a wavelength spacing of f_D is obtained, which is illustrated in Fig. 2(i). Then, the dual-λ laser source is sent to the ring modulator through a polarisation controller (PC, PC_1). When properly setting the dual-λ laser source according to the response obtained in Fig. 1*b*, one of the carriers of the dual-λ laser source will align to the resonant wavelength of the ring modulator. Thus, only one of the optical carriers will be modulated by the intermediate frequency (IF) downstream data applied to the ring modulator, while the other one remains unmodulated. In this way, an SSB-modulated optical downstream signal is generated, as shown in Fig. 2(ii). After passing through an optical circulator (OC, OC_1), the SSB-modulated optical downstream signal is transmitted to the RRH via optical single-mode fibre (SMF).

In the RRH, the incoming optical signal goes through another OC (OC_2) and is split into two portions. One portion is directly sent to a photodetector (PD, PD_1), from which an RF signal with a carrier frequency f_D is obtained, as can be seen from Fig. 2(iii). To realise the full-duplex communication, the unmodulated optical carrier in the other portion of the optical downstream signal is extracted by an optical bandpass filter (OBPF, Santec OTF350) and modulated by a 10-GHz MZM via a second PC (PC_2). Fig. 2(v) shows the upstream

signal after being modulated with the upstream data at a carrier frequency of f_U. The optical upstream signal is transmitted back to the CO, after passing through OC_2, SMF and OC_1, respectively. In the CO, the optical upstream signal is detected by another PD (PD_2) resulting in the electrical upstream signal shown in Fig. 2(vi).

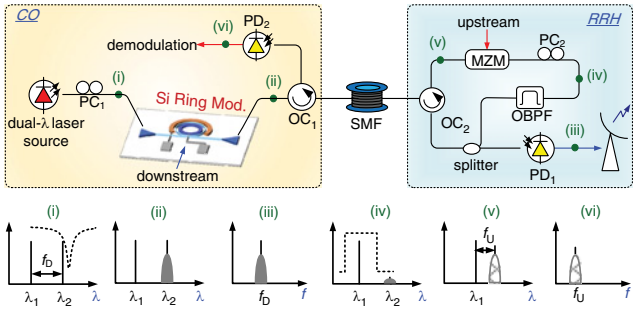

Fig. 2 *Schematic diagram of the proposed full-duplex RoF system based on an integrated silicon ring modulator. (i)–(vi): illustrations of the optical spectra at different points of the system*

The downstream and upstream data are generated by a four-channel arbitrary waveform generator (Keysight M9052A). The electrical spectra are observed by an electrical spectrum analyser (Agilent N9010A), and the data are demodulated by a real-time oscilloscope (Keysight DSA-Z 634A).

Experiment results: In our experiment, the wavelength spacing, i.e. f_D, of the dual-λ laser source is set to be 20 GHz. For the downstream link, a 1-GHz IF signal carrying 250-Mbaud 16QAM data (i.e. 1-Gb/s data rate) is applied to the ring modulator. Fig. 3*a* shows the electrical spectrum measured at the output of PD_1. As can be seen from the electrical spectrum, due to the frequency beating between the unmodulated and the modulated optical carriers of the dual-λ laser source, the 1-GHz IF signal is upconverted to the 21 GHz band. The insets of Fig. 3*a* show a zoom-in of the spectrum and the corresponding constellation diagram of the demodulated 16QAM data. The measured EVM evaluated by 1000 symbols is 4.3%. Fig. 3*b* shows the measured EVM versus the received optical power for the back-to-back (b2b) signal and for a 5-km downstream link. As can be seen, for a received optical power of −18 dBm, the EVM is lower than 5%. Furthermore, owing to the SSB modulation of the downstream link, the fibre transmission link introduces a negligible deterioration in the EVM. Owing to the limited facilities in our lab, the fibre length is restricted to be 5 km in our experiment. However, we believe that the fibre length can be further increased thanks to the SSB modulation.

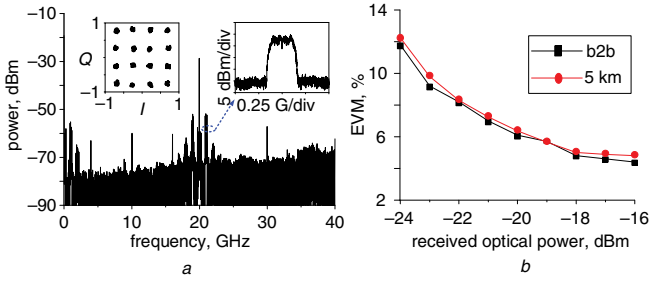

Fig. 3 *Transmission performances of the downstream link*

a Electrical spectrum of the downstream signal obtained in the RRH
b EVM versus received optical power for back-to-back (b2b) and 5-km downstream link

For the upstream link, the unmodulated optical carrier in the optical downstream signal is selected by the OBPF in the RRH and re-modulated by a 10-GHz RF signal carrying 50-Mbaud 16QAM data. The electrical spectrum obtained at the output of PD_2 in the CO is shown in Fig. 4*a*. The corresponding constellation diagram is shown as the inset in Fig. 4*a* with an EVM evaluated by 1000 symbols of 3.5%. Fig. 4*b* shows the measured relationship between the EVM and the received optical power for the upstream link. As can be seen, when the received optical power is larger than −7 dBm, the EVM is lower than 5%.

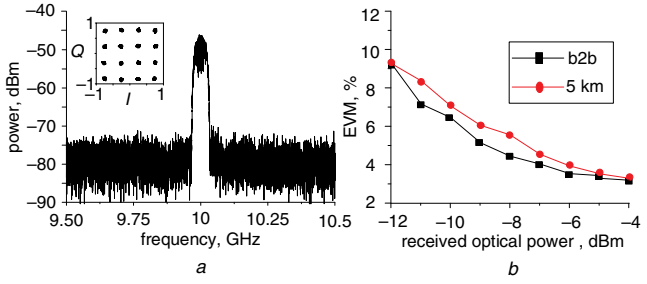

Fig. 4 *Transmission performances of the upstream link*

a Electrical spectrum of the downstream signal obtained in the CO
b EVM versus received optical power for b2b and 5-km upstream link

The sensitivity of the EVM to the bias voltage applied to the silicon ring modulator is also investigated. The EVM versus the received optical power of the downstream link at different bias voltages is depicted in Fig. 5. As can be seen, the transmission performance is dependent on the bias voltages applied to the ring modulator, so bias control is necessary to reduce this influence.

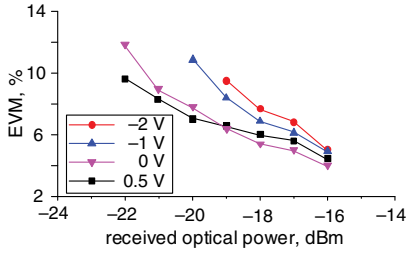

Fig. 5 *Measured EVM versus the received optical power of the downstream link at different bias voltages of the ring modulator*

It is worth noting that the MZM used for the dual-λ laser source generation can be integrated with the ring modulator into a single chip to make the system cheaper and more compact [17]. It should also be noted that many other schemes can be used to produce the dual-λ laser source, such as a dual-mode optical laser [18], an integrated heterodyne distributed feedback (DFB) laser [19], or two optical tones selected from a frequency comb [20]. By adjusting the spacing of the dual-λ laser source, the RF carrier can be easily increased to the higher frequency band (e.g. 60 GHz or THz band). In addition, limited by the analysis bandwidth of the signal analyser, 250-MBaud 16-QAM data is demonstrated in the proposed system. However, since the bandwidth of the silicon ring modulator is 15 GHz and is possible to be increased to >40 GHz if imec's newest iSIPP50G platform is applied, the data-rate of the downstream link can be significantly improved.

Conclusion: In this Letter, based on an integrated silicon ring modulator and a centralised optical dual-λ laser source, we have proposed and demonstrated a low-cost full-duplex RoF system with local SSB modulation to reduce the fibre dispersion influence, and remote carrier reuse to avoid the usage of the laser source in the remote head. EVM<5% for both the 21-GHz downstream and 10-GHz upstream links is achieved in a proof-of-concept experiment. The sensitivity to the bias voltage of the ring modulator is also evaluated. The proposed architecture shows a possible low-cost solution for future high-frequency (60 GHz or beyond) and high-speed (several tens of Gb/s) wireless communication systems.

Acknowledgments: This work was supported by in part by H2020 TOPHIT project, the National Natural Science Foundation of China (61527820) and the Fundamental Research Funds for the Central Universities. Z.Z. Tang would also like to thank the support of the China Scholarship Council (CSC).

Submitted: *09 May 2019* E-first: *7 August 2019*
doi: 10.1049/el.2019.1630
One or more of the Figures in this Letter are available in colour online.

Zhenzhou Tang, Jing Zhang, Gunther Roelkens and Dries Van Thourhout (*Photonics Research Group, Department of Information Technology, Ghent 9052, imec, Leuven 3001, Belgium*)

Shilong Pan (*Key Laboratory of Radar Imaging and Microwave Photonics, Ministry of Education, Nanjing University of Aeronautics and Astronautics, Nanjing 210016, People's Republic of China*)

✉ E-mail: pans@nuaa.edu.cn

Zhenzhou Tang, Jing Zhang, Gunther Roelkens and Dries Van Thourhout: Also with Center for Nano- and Biophotonics, Ghent 9000, Belgium

Zhenzhou Tang: Also with Key Laboratory of Radar Imaging and Microwave Photonics, Ministry of Education, Nanjing University of Aeronautics and Astronautics, Nanjing 210016, People's Republic of China

References

1 Wang, C.X., Haider, F., Gao, X., *et al.*: 'Cellular architecture and key technologies for 5G wireless communication networks', *Commun. Mag.*, 2014, **52**, (2), pp. 122–130
2 Wu, J., Zhang, Z., Hong, Y., *et al.*: 'Cloud radio access network (C-RAN): a primer', *Netw.*, 2015, **29**, (1), pp. 35–41
3 Tang, Z.Z., Zhang, F.Z., and Pan, S.L.: '60-GHz RoF system for dispersion-free transmission of HD and multi-band 16QAM', *Photon. Technol. Lett.*, 2018, **30**, (14), pp. 1305–1308
4 Zhang, L., Udalcovs, A., Lin, R., *et al.*: 'Toward terabit digital radio over fiber systems: architecture and key technologies', *Commun. Mag.*, 2019, **57**, (4), pp. 131–137
5 Tang, Z.Z., and Pan, S.L.: 'A full-duplex radio-over-fiber link based on a dual-polarization Mach–Zehnder modulator', *Photon. Technol. Lett.*, 2016, **28**, (8), pp. 852–855
6 Tang, Z.Z., and Pan, S.L.: 'A Q-band radio-over-fiber system for distribution of uncompressed high-definition video signals', *Photonic Netw. Commun.*, 2016, **32**, (2), pp. 179–187
7 Nanni, J., Tegegne, Z.G., Algani, C., *et al.*: 'Use of SiGe phototransistor in RoF links based on VCSEL and standard single mode fiber for low cost LTE applications'. Int. Topical Meeting on Microwave Photonics (MWP), Toulouse, France, October 2018, pp. 1–4
8 Gasse, K.Van, Bogaert, L., Breyne, L., *et al.*: 'Analog radio-over-fiber transceivers based on III–V-on-silicon photonics', *Photon. Technol. Lett.*, 2018, **30**, (21), pp. 1818–1821
9 Gasse, K.Van, Kerrebrouck, J.Van, Abbasi, A., *et al.*: 'III-V-on-silicon photonic transceivers for radio-over-fiber links', *J. Lightw. Technol.*, 2018, **36**, (19), p. 4438
10 Huang, M.H., Li, S.M., Xue, M., *et al.*: 'Flat-top optical resonance in a single-ring resonator based on manipulation of fast- and flow-light effects', *Opt. Express*, 2018, **26**, (18), pp. 23215–23220
11 Manganelli, C.L., Pintus, P., Gambini, F., *et al.*: 'Large-FSR thermally tunable double-ring filters for WDM applications in silicon photonics', *Photon. J.*, 2017, **9**, (1), pp. 1–10
12 Gasse, K.Van, Verbist, J., Li, H., *et al.*: 'Silicon photonics radio-over-fiber transmitter using GeSi EAMs for frequency up-conversion', *Photon. Technol. Lett.*, 2019, **31**, (2), pp. 181–184
13 Park, J., Sorin, W.V., and Lau, K.Y.: 'Elimination of the fibre chromatic dispersion penalty on 1550 nm millimetre-wave optical transmission', *Electron. Lett.*, 1997, **33**, (6), pp. 512–513
14 Smith, G.H., Novak, D., and Ahmed, Z.: 'Technique for optical SSB generation to overcome dispersion penalties in fibre-radio systems', *Electron. Lett.*, 1997, **33**, (1), pp. 74–75
15 Shao, T., Paresys, F., Le Guennec, Y., *et al.*: 'Convergence of 60 GHz radio over fiber and WDM-PON using parallel phase modulation with a single Mach–Zehnder modulator', *J. Lightw. Technol.*, 2012, **30**, (17), pp. 2824–2831
16 Omomukuyo, O., Thakur, M.P., and Mitchell, J.E.: 'Simple 60-GHz MB-OFDM ultrawideband RoF system based on remote heterodyning', *Photon. Technol. Lett.*, 2013, **25**, (3), pp. 268–271
17 Tong, Y., Chow, C-.W., Chen, G-.H., *et al.*: 'Integrated silicon photonics remote radio frontend (RRF) for single-sideband (SSB) millimeter-wave radio-over-fiber (RoF) systems', *Photon. J.*, 2019, **11**, (2), p. 7202108
18 Chen, X., Deng, Z., and Yao, J.P.: 'Photonic generation of microwave signal using a dual-wavelength single-longitudinal-mode fiber ring laser', *Trans. Microw. Theory Tech.*, 2006, **54**, (2), pp. 804–809
19 Mu-Chieh, L., Zarzuelo, A., Guzmán, R., *et al.*: 'Foundry-fabricated heterodyne DFB laser microchip for 600 MHz – 23 GHz RF generation'. 48th European Microwave Conf. (EuMC), Madrid, Spain, September 2018, pp. 793–795
20 Browning, C., Martin, E.P., Farhang, A., *et al.*: '60 GHz 5g radio-over-fiber using UF-OFDM with optical heterodyning', *Photon. Technol. Lett.*, 2017, **29**, (23), pp. 2059–2062